Circulation: Arrhythmia and Electrophysiology

ORIGINAL ARTICLE

Simultaneous Comparison of Electrocardiographic Imaging and Epicardial Contact Mapping in Structural Heart Disease

BACKGROUND: The accuracy of ECG imaging (ECGI) in structural heart disease remains uncertain. This study aimed to provide a detailed comparison of ECGI and contact-mapping system (CARTO) electrograms.

METHODS: Simultaneous epicardial mapping using CARTO (Biosense-Webster, CA) and ECGI (CardioInsight) in 8 patients was performed to compare electrogram morphology, activation time (AT), and repolarization time (RT). Agreement between AT and RT from CARTO and ECGI was assessed using Pearson correlation coefficient, ρ_{AT} and ρ_{RT}, root mean square error, E_{AT} and E_{RT}, and Bland-Altman plots.

RESULTS: After geometric coregistration, 711 (439–905; median, first-third quartiles) ECGI and CARTO points were paired per patient. AT maps showed ρ_{AT}=0.66 (0.53–0.73) and E_{AT}=24 (21–32) ms, RT maps showed ρ_{RT}=0.55 (0.41–0.71) and E_{RT}=51 (38–70) ms. The median correlation coefficient measuring the morphological similarity between the unipolar electrograms was equal to 0.71 (0.65–0.74) for the entire signal, 0.67 (0.59–0.76) for QRS complexes, and 0.57 (0.35–0.76) for T waves. Local activation map correlation, ρ_{AT}, was lower when default filters were used (0.60 (0.30–0.71), P=0.053). Small misalignment of the ECGI and CARTO geometries (below ±4 mm and ±4°) could introduce variations in the median ρ_{AT} up to ±25%. Minimum distance between epicardial pacing sites and the region of earliest activation in ECGI was 13.2 (0.0–28.3) mm from 25 pacing sites with stimulation to QRS interval <40 ms.

CONCLUSIONS: This simultaneous assessment demonstrates that ECGI maps activation and repolarization parameters with moderate accuracy. ECGI and contact electrogram correlation is sensitive to electrode apposition and geometric alignment. Further technological developments may improve spatial resolution.

VISUAL OVERVIEW: A visual overview is available for this article.

Adam J. Graham, MRCP*
Michele Orini, PhD*
et al

*Drs Graham and Orini are joint first authors.

The full author list is available on page 9.

Key Words: activation and repolarization maps ■ contact mapping ■ ECG imaging ■ unipolar electrograms ■ ventricular tachycardia

https://www.ahajournals.org/journal/circep

WHAT IS KNOWN?

- ECG imaging (ECGI) allows noninvasive reconstruction of epicardial unipolar electrograms using body surface potentials in just 1 beat.
- The ECGI system has been recently introduced for clinical application, and its accuracy has not been assessed with simultaneous recordings during catheter ablation for ventricular tachycardia.
- A recent study has shown that the correlation between sinus rhythm activation time maps between ECGI and contact mapping is lower than what previously reported in experimental conditions using research-based algorithms.

WHAT THE STUDY ADDS?

- We found moderate correlation between activation-repolarization maps and signal morphology from contact versus noncontact mapping during ventricular pacing.
- ECGI localizes sites of epicardial focal activation with a resolution of 13.2 (0.0–28.3) mm.
- We highlight the intrinsic difficulty of validation studies and calculate that small changes in the geometric alignment between ECGI geometry and electroanatomical maps could result in up to a ±25% change in correlation between activation time maps.

ECG imaging (ECGI) utilizes body surface potentials and heart-torso geometries to reconstruct epicardial unipolar electrograms. This is achieved applying an inverse solution and provides insight into the electrophysiological substrate customarily only delineated with invasive contact electroanatomical mapping (EAM).[1,2]

The ability to delineate whole tachycardia circuits using a single beat has important implications for hemodynamically unstable ventricular tachycardias (VTs), which cannot be easily mapped using EAM.[3] Furthermore, this technology could facilitate risk stratification in primary prevention implantable cardioverter defibrillator candidates.[4,5]

Initial experimental validation of the methodology utilizing a tank-torso model showed its ability to image cardiac activation and repolarization,[2,6,7] which was confirmed in open chest canines versus contact electrogram data.[8] Human work during cardiac surgery showed promising results, although contact and ECGI maps were not acquired simultaneously.[9] This has culminated in the use of the system for ablation of focal ectopy, VT, atrial fibrillation,[10,11] and noninvasive ablation of ventricular arrhythmias with radiotherapy.[12,13]

However, despite the range of clinical applications, there has been no direct quantitative simultaneous comparison to contact electrogram data in the intact human heart. Simultaneous collection of epicardial contact and body surface ECGI data in canine and porcine models showed moderate correlation for activation time (AT) and repolarization time (RT).[14,15] In humans, using a 120 lead system, simultaneous contact electrical data demonstrated variable accuracy for locating epicardial pacing sites and qualitatively assessed ventricular activation sequences.[16] Nonsimultaneous mapping recently showed ECGI reconstruction of activation sequences was poor during sinus rhythm with a narrow QRS complex.[17]

This study set out to prospectively compare simultaneously recorded epicardial contact electrograms with reconstructed epicardial electrograms from a 252 electrode ECGI system (CardioInsight, Medtronic, MN) in the intact human heart.

METHODS

The authors declare that all supporting data are available within the article and its Data Supplement. The raw data that support the findings of this study are available from the corresponding author on reasonable request. Eight patients (5 male, 3 female), aged 45.9±15.5 years undergoing epicardial catheter ablation of structurally abnormal heart VT were studied with ECGI mapping during ablation. All patients were scheduled for a catheter ablation procedure on clinical grounds and gave their informed consent to participate in the research study. The study was approved by the National Research Service Committee, London (14/LO/0360).

Clinical Procedure

Procedures were performed with the patient under general anesthesia. Endocardial access was obtained under ultrasound guidance using Seldinger technique via the right femoral vein±right femoral artery. A subxiphisternal puncture using a Tuohy needle, with fluoroscopic guidance, was used to access the epicardial space.[18] An EAM (CARTO, Biosense-Webster, CA) of the epicardial surface was created during right ventricular (RV) pacing in 6 patients, biventricular pacing in 1 patient, and atrial pacing in another. This was to ensure stable rhythms for electrogram data collection. For the latter 2 patients, pacing modalities were chosen to improve hemodynamic status during mapping. A multipolar catheter (Pentarray or Decapolar, Biosense-Webster, CA) was used for all cases. Unipolar electrograms were collected from all points during EAM creation with band-pass filters set at 0.05 Hz to 500 Hz and a sampling frequency of 1000 Hz. Pacing was performed from multiple locations on the epicardium at <10 mA.

ECGI Recordings

Before catheter ablation, a 252 electrode vest (CardioInsight, Medtronic, MN) was fitted for recording of body surface potentials (sampling rate 1000 Hz) and remained in situ until conclusion of the procedure. A noncontrast axial computed tomography scan with 3-mm slice thickness was performed up to 4 hours before the procedure. Patient-specific epicardial geometry was created using the EcVue system (Medtronic, MN) with data from the computed tomography and body surface

potentials. Epicardial unipolar electrograms were computed over ≈1400 epicardial points covering both ventricles using both unfiltered and filtered (low pass 50 Hz) data, with those over the atrioventricular valves manually excluded. A full aortic mesh, comprising the ascending, arch, and descending portions, was created in patients with arterial access. If arterial access was not obtained, a detailed geometry of the RV outflow tract, inferior vena cava, and superior vena cava was generated.

Data Analysis

Unipolar electrograms from CARTO and ECGI were independently analysed with bespoke software (Matlab, The Mathworks, Inc, MA). After pacing artifact removal, signals were band-pass filtered between 0.5 and 80 Hz for AT measurement and between 0.5 and 20 Hz for RT measurement. AT was measured as the time of the steepest signal downslope (dV/dt_{min}) during the QRS complex and RT the time of steepest upslope (dV/dt_{max}) during the T wave.[19,20] All signals were carefully reviewed and semiautomatically corrected if needed as in previous studies.[21,22]

Coregistration of EAM and ECGI geometries was performed semiautomatically with bespoke software (Matlab, The Mathworks, Inc, MA). As Figure 1 shows, accuracy was achieved by simultaneous alignment of all prominent anatomic geometries including the aorta (in 4 patients) and inferior vena cava and RV outflow tract (in 4 patients). The optimal coregistration was visually determined by 2 experts independent of subsequent analysis. After coregistration, for each point belonging to the ECGI geometry, the closest point belonging to the CARTO geometry was found, and the 2 points were paired for comparison. ECGI and CARTO points were paired only if their Euclidean distance was lower than D=8 mm. To reduce the effect of outliers, spatial smoothing was performed by averaging AT and RT of points contained within a D=8 mm radius. The analysis was repeated for D ranging from 5 to 14 mm to assess the impact of spatial smoothing on the results. To assess the sensitivity of our results to coregistration between ECGI and CARTO geometries, the analysis was repeated after applying small changes to the optimal coregistration. In total, the analysis was repeated 4096 times per patient consistent with all possible configurations obtained by applying a shift of –4, –2, +2 and +4 mm and a rotation of –4°, –2°, +2°, and +4° along and around the 3 major axes.

To assess spatial resolution of the localization of earliest sites of epicardial activation, the minimum Euclidean distance between the pacing pole (projected onto the ECGI ventricular geometry) and the region of earliest activation (within the first-fifth percentile) in the ECGI map was measured. The interval from stimulus to QRS was calculated for each pacing beat. Beats were then separated into those with an interval from stimulus to QRS of <40 and >40 msec.

Statistical Analysis

Data distribution is described by median (first-third quartiles). Statistical differences were assessed using the Wilcoxon rank-sum test for unpaired comparisons and the Wilcoxon signed-rank test for paired comparisons. Threshold for statistical significance was 0.05. The morphological similarity between each pair of signals was assessed using Pearson correlation coefficient (CC). The agreement of activation and repolarization sequences between the 2 modalities was quantified with the root mean square error, Pearson CC, and Bland-Altman plots. Interpatient correlations between, for example, the CC for AT or RT maps and QRS duration, QRS amplitude, or number of electrodes in contact with the body surface were assessed using Spearman CC. Data and statistical analyses were conducted in MATLAB, MathWorks.

RESULTS

Eight patients were studied. Five were elective procedures with the remaining 3 in-patient emergency procedures. Baseline characteristics can be seen in Table 1. The prevalence of arrhythmogenic RV cardiomyopathy cases accounted for by the epicardial nature of this condition.

Activation and Repolarization Maps

Three thousand seven hundred and ninety (1845–6022; median, Q1–Q3) and 1385 (1362–1395) unipolar sig-

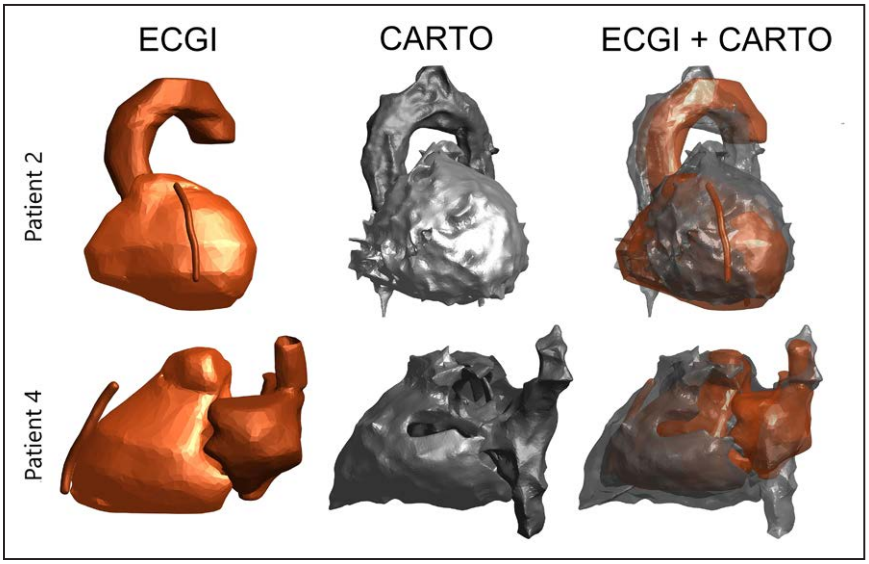

Figure 1. Anatomical coregistration of ECG imaging (ECGI) and CARTO geometries in 2 patients.
ECGI and CARTO geometries are shown on the **left** and in the **middle**, respectively, and they are combined in a unified reference system on the **right**. Patient 2 is displayed in left anterior oblique and patient 4 in left lateral view.

Table 1. Baseline Characteristics

Patient	Age	Sex	Pathogenesis	Rhythm	Anatomic Structure	UEG CARTO Signals	Pacing Maps
1	46	Female	ARVC	RV pacing	RVOT	6289	No
2	73	Male	IHD	Bi-V pacing	Aorta	3007	Yes
3	48	Male	BrS	RV pacing	Aorta	2614	Yes
4	24	Female	ARVC	RV pacing	RVOT	5755	No
5	43	Male	DCM	RV Pacing	Aorta	6610	No
6	52	Female	ARVC	RV pacing	RVOT	1077	Yes
7	58	Male	ARVC	RV pacing	RVOT	4573	Yes
8	21	Male	DCM	A pacing	Aorta	619	No

A indicates atria; ARVC, arrhythmogenic right ventricular cardiomyopathy; Bi-V, bi-ventricular; BrS, Brugada syndrome; DCM, dilated cardiomyopathy; IHD, ischaemic heart disease; RV, right ventricular; RVOT, right ventricular outflow tract; and UEG, unipolar electrogram.

nals per patient from CARTO and ECGI, respectively, were used for the analysis. Of these, 711 (439–905) per patient were paired and used for comparison. Figures 2 and 3 show examples of AT and RT maps produced by the 2 systems for comparison, whereas numerical results are shown in Table 2. Visually, there was consistency between ECGI and EAM maps. CC measuring the similarity of AT and RT sequences was equal to 0.66 (0.53–0.73) for AT and 0.55 (0.41–0.72) for RT, whereas root mean square error was equal to 24 (21–35) ms for AT and 51 (38–70) ms for RT. Seven of 8 patients had a CC for AT sequence higher than 0.5. Scatter-plots and Bland-Altman plots showing inter-modality agreement for AT and RT per each patient are shown in Figures I through VIII in the Data Supplement. The CC for AT maps showed moderate correlation with QRS duration (ρ=0.52), suggesting that slower AT sequences can be noninvasively mapped more reliably and with mean QRS amplitude of the 12 leads ECG (ρ=0.65, excluding the 1 patient with atrial pacing),

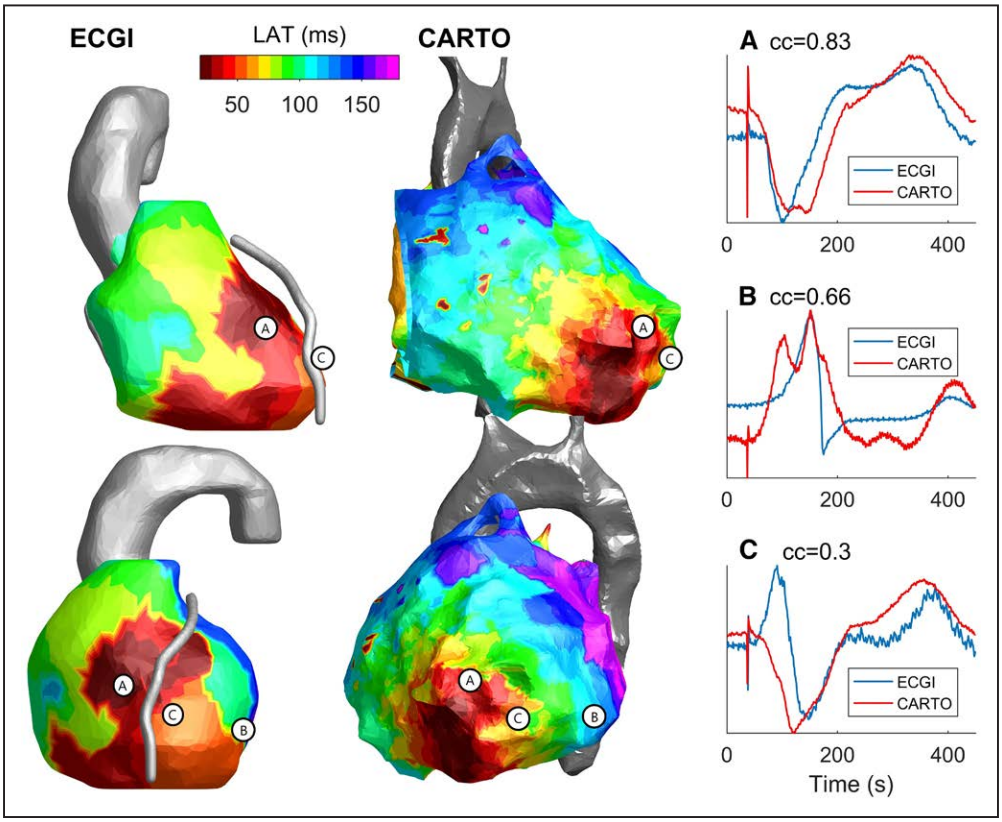

Figure 2. Comparison of activation times during right ventricular (RV) pacing for ECG imaging (ECGI) and CARTO.
Images on **top** are seen in right lateral view and the **bottom** ones in left anterior oblique. Area of earliest activation is displayed in red with purple representing areas of latest activation. Labels A, B, and C on the geometry corresponds to sites where morphological similarity of QRS complexes is high (A, correlation coefficient [cc]=0.83, 75th percentile of ccs), good (B, cc=0.66, median correlation), and low (C, cc=0.30, 25th percentile of ccs). Unipolar electrograms are shown on the **right** (**A**–**C**). LAT indicates local activation time in milliseconds.

Table 2. Agreement Between ECGI and Contact Mapping

Patient Data	N-el (n)	QRS (ms)	Pairs (n)	ρAT (n.u.)	ρRT (n.u.)	EAT (ms)	ERT (ms)	ρ^{med}_{QRS} (n.u.)	ρ^{med}_{TW} (n.u.)	ρ^{med}_{UEG} (n.u.)
Patient										
1	207	155	890	0.76	0.72	25	62	0.68	0.45	0.71
2	218	153	727	0.67	0.59	45	78	0.59	0.44	0.61
3	201	164	584	0.80	0.50	24	55	0.67	0.80	0.69
4	175	95	919	0.65	0.69	23	29	0.75	0.71	0.78
5	179	110	926	0.51	0.33	27	46	0.60	0.69	0.71
6	172	101	232	0.69	0.84	18	19	0.78	0.80	0.78
7	175	123	694	0.29	0.30	36	103	0.24	-0.11	0.23
8	181	98	285	0.54	0.51	15	48	0.78	0.26	0.71
Statistics										
Mean	189	125	657	0.62	0.56	27	55	0.63	0.51	0.65
SD	18	28	274	0.16	0.19	10	27	0.18	0.32	0.18
Quartiles										
First Q	175	100	435	0.53	0.41	21	38	0.59	0.35	0.65
Median	180	117	711	0.66	0.55	24	51	0.67	0.57	0.71
Third Q	204	154	905	0.73	0.71	32	70	0.76	0.76	0.74

N-el denotes number of body-surface electrodes used for ECGI calculation; QRS, QRS duration in ms; Pairs, number of epicardial points with simultaneous ECGI and CARTO data. E_{AT} *and* E_{RT} indicates root mean square error for activation and repolarization times; ECGI, ECG imaging; ρ_{AT} and ρ_{RT}, correlation coefficients for activation and repolarization times; ρ^{med}_{QRS}, ρ^{med}_{TW}, ρ^{med}_{UEG}, morphological correlation coefficient measured within the QRS, T waves, and entire signals, respectively; n, number; n.u., normalized units; Q, quartile; and UEG, unipolar electrogram.

suggesting that structural heart disease and low-signal amplitude may reduce mapping accuracy. The number of body surface potentials included in the computation of the inverse problem also showed moderate correlation with CC for AT maps (ρ=0.40), indicating that care should be taken in maintaining good contact between the ECGI vest and patient's torso. The CC for AT maps decreased from 0.66 (0.53–0.73) to 0.60 (0.30–0.7), *P*=0.053 if the body surface potentials were low-pass filtered using the by default filter setting of the CardioInsight system before reconstructing the epicardial potentials.

Signal Morphology

The CC measuring the morphological similarity between unipolar electrograms recorded with contact mapping and computed with ECGI was equal to 0.71 (0.65–0.74) when considering the entire duration of the signal and equal to 0.67 (0.59–0.76) within the QRS complex and 0.57 (0.35–0.76) for the T wave (see Table 2). Seven of 8 patients had a morphological CC for the QRS complex higher than 0.5. These results were not significantly different when computed using prefiltered data. Figures IX through XVI in the Data Supplement show the distribution of the CC and representative electrogram examples going from best to worst correlation. There was a marked intrapatient variability in the CCs measuring morphological similarity between recorded and computed electrograms, with median interquartile range equal to 0.67.

Localization of Earliest Sites of Activation

In Figure 4 examples of localization of pacing sites on the EAM to the area of earliest activation on ECGI map are shown for 3 representative patients. The white circle represents the pacing site projected onto the ECGI geometry. Table 3 shows distance for pacing site accuracy in all patients.

Overall, the distance from n=46 epicardial pacing sites to the corresponding areas of earliest activation was 20.7 (9.6–33.2) mm. This was significantly lower for the n=25 pacing sites for which local capture was confirmed by a short stimulus to QRS interval, with distance equal to 13.2 (0.0–28.3) mm for stimulus to QRS interval ≤40 ms versus 32.6 (21.5–45.8) mm (*P*<0.001) for stimulus to QRS interval >40 ms.

Agreement Between EAM and ECGI in Low-Voltage Regions

Low-voltage regions were defined as cardiac sites for which EAM registered a bipolar signal amplitude <0.5 mV. Indices of agreement between EAM and ECGI calculated in low-voltage regions were not different from those calculated in normal voltage regions (Table I in the Data Supplement). Pacing sites were considered as

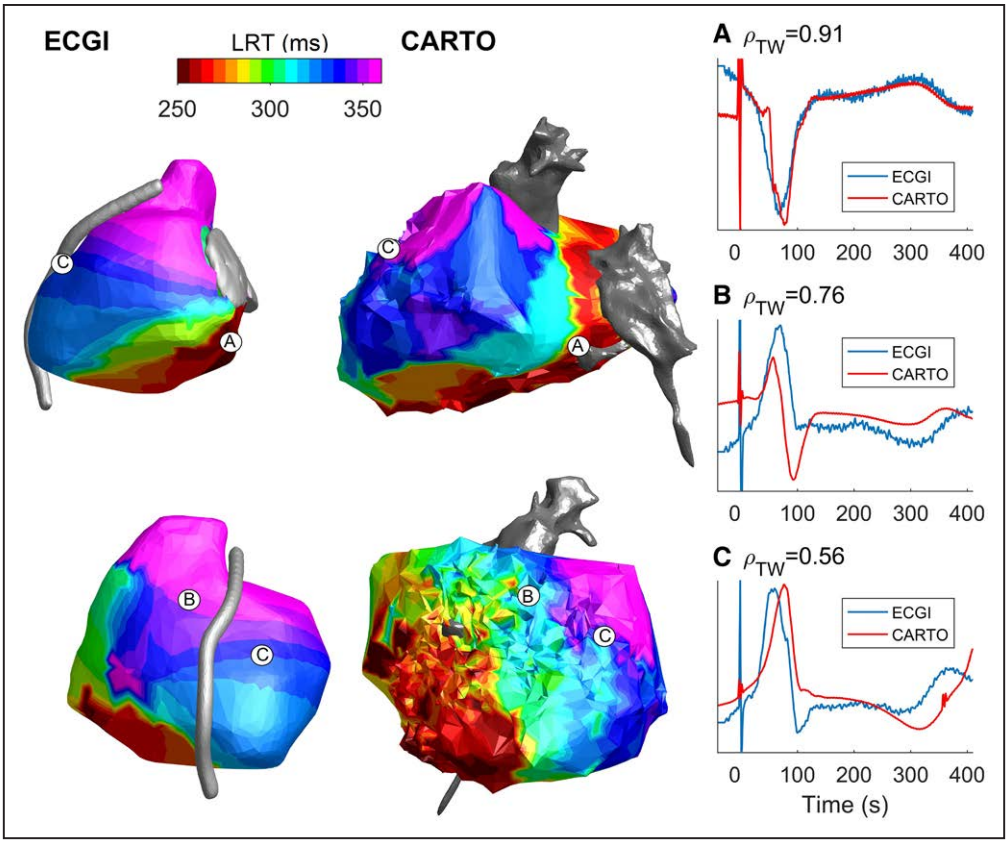

Figure 3. Comparison of repolarization time maps from ECG imaging (ECGI) and CARTO in a representative patient.
The **top** pictures are in left lateral view and the **bottom** in left anterior oblique. The left anterior descending artery is displayed for orientation and demarcation of left and right ventricles. Early repolarization is in red and late in purple. Labels A, B, and C on the geometry corresponds to sites where morphological similarity of the T-wave of the unipolar electrogram is high (A, correlation coefficient [cc]=0.91, 75th percentile of ccs), good (B, cc=0.76, median correlation), and low (C, cc=0.56, 25th percentile of ccs). Unipolar electrograms at these sites are shown on the **right** (**A**–**C**). LRT indicates local repolarization time in milliseconds.

belonging to a low-voltage region if the median bipolar amplitude recorded with EAM within a search radius equal to 4 mm was <0.5 mV. The distance between pacing sites and the regions of earliest activation in ECGI was not different when comparing pacing sites in low- versus normal-voltage regions (Table II in the Data Supplement).

Effects of Anatomic Coregistration

Parameter *D*, which corresponds to the minimum distance used for pairing cardiac sites from EAM and ECGI maps and determines the amount of spatial smoothing did not have a significant impact on the results (Figure XVII in the Data Supplement). However, small variations in the anatomic coregistration may have an impact on the results. Although on average the agreement between ECGI and CARTO AT maps (ρ_{AT}) did not change after applying small changes to the optimal anatomic coregistration (Table II in the Data Supplement), the selection of the configuration that for each patient maximizes or minimizes ρ_{AT} (Figures XVIII through XXV in the Data Supplement for comparison) would have resulted in a ±25% variation of the median ρ_{AT} (Table I in the Data Supplement).

DISCUSSION

This is the first quantitative comparison of reconstructed electrograms using ECGI versus simultaneously recorded contact epicardial data in the intact human heart.

The main findings are as follows: morphological comparison between recorded and computed unipolar electrograms shows median CC per patient equal to 0.71 (0.65–0.74); AT maps showed a correlation of ρ_{AT}=0.66 (0.53–0.73) and mean squared error of E_{AT}=24 (21–32) ms; and RT maps showed ρ_{RT}=0.55 (0.41–0.71) and E_{RT}=51 (38–70) ms. Minimum distance between epicardial pacing sites and the region of earliest activation in ECGI was 13.2 (0.0–28.3) mm for pacing sites where a short stimulus to QRS interval confirmed local capture. This quantitative assessment is sensitive to anatomic coregistration.

Overall these data suggest that the accuracy of the noninvasive mapping system may not provide sufficient resolution to guide radiofrequency ablation of ventricular arrhythmias but could shorten and potentially improve the efficiency of ablation procedures by allowing rapid targeting for contact mapping focal ectopics or in situations of hemodynamic instability.

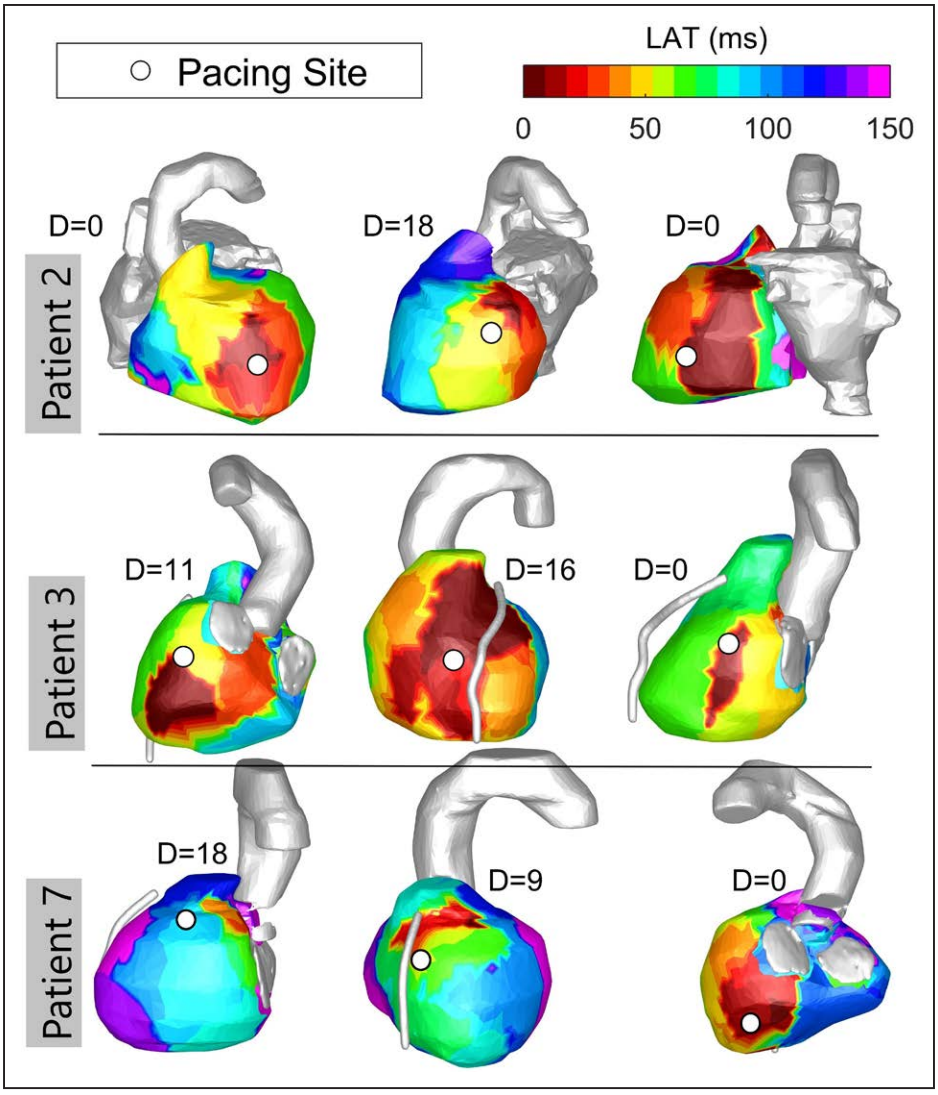

Figure 4. Relation between pacing site location as defined by CARTO position at time of pacing (white circles) and ECGI maps of activation time. Three patients are included with 3 pacing sites for each. Area of early activation is in red with late activation in purple. Distance between pacing site and region of earliest activation (D) is reported next to each map. LAT indicates local activation time in milliseconds.

The correlations reported in this study are similar to those demonstrated in proof-of-principle studies. Initial experiments using the tank-torso model found a CC of 0.81 for AT,[6] but the tank-torso model does not take into account motion artifact during respiration or the effect of lung tissue between the epicardium and body surface electrodes.[23]

A CC of 0.72 for AT was found in cardiac surgery patients using consecutive and not simultaneously recorded data.[9] More recently, a canine model, under closed-chest conditions, found a median CC of 0.73 for AT.[14] Although these data show higher correlation than 0.66 we observed, our data are the first simultaneously recorded quantitative clinical data taken during an ablation procedure. Our results are comparable to a simultaneous ECGI epicardial sock closed-chest porcine study showing mean CCs for reconstructed epicardial potential distributions ranged from 0.60±0.08 to 0.64±0.07 and general activation spread median CC 0.72–0.78 for AT maps after spatiotemporal smoothing.[15]

Our results contrast with recently published data comparing ECGI and EAM in 55 patients, where AT was found to be largely inaccurate (CC 0.03±0.43).[17] Mapping was performed mainly during sinus rhythm, with better correlation seen during paced rhythms. The study used the commercially available system for production of AT maps. The lower values could reflect the methods used to create ECGI maps and the fact that bipolar electrograms from EAM were utilized without direct cross-correlation with the corresponding unipolar contact signals which could be a further source of erroneous measurement. We used bespoke software to analyse the electrograms along with manual editing. In our experience, significant editing of the electrograms is required to ensure accurate annotation of

Table 3. Distance Between Pacing Site and Earliest Region of Activation in ECGI Maps

	Any S-QRS Interval				S-QRS<40 ms			
Patient	N	Q1 (mm)	Median (mm)	Q3 (mm)	N	Q1 (mm)	Median (mm)	Q3 (mm)
2	4	0.0	6.1	15.0	4	0.0	6.1	15.0
3	17	14.8	31.3	36.3	11	7.9	30.9	32.9
6	8	8.5	22.5	35.5	3	3.4	13.6	23.4
7	17	8.9	19.4	31.7	7	0.0	6.8	12.3
Total	46	9.6	20.7	33.2	25	0.0	13.2	28.3

ECGI indicates ECG imaging; N, number of pacing sites; Q, quartile; and S-QRS, interval from stimulus to QRS.

AT in both contact and noncontact mapping data. We also found moderate association between AT maps correlation and body surface QRS duration (ρ=0.52). This suggests that the accuracy of ECGI activation maps is higher for slower wavefront progression, which has important implications for mapping during narrow QRS rhythms where recent data indicated reduced accuracy of identifying epicardial breakthroughs and location of lines of block by comparison with high-density epicardial mapping.[17] Narrower QRS complexes reflect more rapid myocardial activation utilizing the Purkinje network and are not representative of the slower activation of ventricular arrhythmias and epicardial pacing. Epicardial recruitment would be expected to be slower to enable more accurate mapping by ECGI because larger myocardial segments will be activated simultaneously within the spatio-temporal resolution of the system. Indeed, recent success in targeting of ablation resistant VT circuits using ECGI mapping indicates that resolution may be sufficient for delivering stereotactic radiation for noninvasive VT ablation. VT episodes decreased from 119 (4–292) to 3 (0–31) in 19 patients at 6 months post-treatment.[12,13] This novel methodology has thus far been performed in a single center, and further research will be needed into both its long-term efficacy and the role played by ECGI to guide this ablation modality.

Filter settings on the ECGI system exert significant effects, as local activation map correlation, ρ_{AT}, was significantly lower when default filters were used. This is important as commercially available systems currently automatically apply a low-pass filter of 50 Hz. Optimization of the number of electrodes in good contact with the body surface is also needed as utilizing fewer electrodes may confound results.

To the best of our knowledge, this is the first attempt in humans to quantify the relationship of RT between recorded and reconstructed electrograms. Reconstruction of spatial variation of RT is an important feature of ECGI in the potential risk stratification of arrhythmic risk.[24] Human torso models have shown that myocardial repolarization was accurately reflected by ECGI.[8,25] Our results can be compared with the afore-mentioned canine model which showed CC of 0.6.[14] Correlations are lower than those for AT. This is expected given the smaller amplitude of the T wave, increasing susceptibility to noise and electrogram smoothing introduced by the inverse solution algorithm. Furthermore, as reported in direct porcine study, although the overall electrogram CC between measured and reconstructed epicardial electrograms was ≈0.7, the interquartile ranges were wide. That is, whereas agreement was reasonable in ≈50% of cases, it was much less in the remainder.[15]

Indices of agreement between ECGI and EAM were not different in low voltage as compared to normal voltage regions. This may be explained by the fact that in fibrotic tissue the local component of the unipolar electrogram is small or nonexistent, and the signal is essentially composed of far-field potential,[20] which may be measured by both contact and noncontact systems with moderate correlation.

Localization of Pacing Sites

The minimum distance between epicardial pacing sites and the region of earliest AT in ECGI was 13.2 mm (0.0–28.3) from 25 pacing sites with stimulus to QRS <40 ms. The distances were significantly greater with stimulus to QRS >40 msec. Other research has shown resolution for locating pacing of around 10 mm[9,26,27] with a more contemporary study in humans of <10 mm for both RV and left ventricular endocardial pacing.[28]The only other study to perform a simultaneous epicardial pacing in humans found results in keeping with ours[16] with a decreased distance from pacing site to area of earliest activation when the stimulus to QRS was <40 msec. The distance between pacing sites and the regions of earliest activation in ECGI was not greater in regions where EAM registered low bipolar voltage. As pacing from a low-voltage region was not clearly associated with a long stimulus-to-QRS interval, this may be because of inaccuracies of bipolar amplitude to delineate scar.[29,30]

Geometric Alignment

Small movements in the coregistered geometries can have large effects on correlation. Considering the most extreme cases, shifts of only ±4 mm and rotations within ±4° can result in a variation of the ECGI-EAM AT correlation up to ±25%. This may confound studies exam-

ining the accuracy of ECGI and should be considered in future research protocols to ensure optimal coregistration of geometries.

Limitations

This study compared contact EAM to ECGI provided by the CardioInsight system as used in the cath lab during VT catheter ablation, and results may not be easily extended to other ECGI methods.[31] This study focused on epicardial mapping during pacing and, hence, cannot be applied to sinus rhythm where activation sequences and breakthroughs from the endocardium may differ. Pacing was used to ensure stable activation and repolarization during sequential mapping, and every precaution was taken to collect captured beats. However, the EAM consists of many beats collected over a few minutes and ECGI uses a single beat. Although all beats were carefully aligned off-line with custom software and manually checked, variation may occur in AT and RT over the course of this period. Recent studies have demonstrated that repeated mapping with different catheters[32] or even with the same catheter but different activation wavefronts[29] may introduce significant differences in the delineation of the arrhythmogenic substrate. In this sense, it is not surprising to register differences between EAM and ECGI and our use of mapping catheters with slightly different configuration and intraelectrode distance (Pentarray and Decapolar) may have affected the comparison between EAM and ECGI data.

Only one full EAM was produced during pacing, which was delivered from the RV apex in all except 2 patients. Further studies should assess the effect of different pacing sites and wavefront directions on the agreement between EAM and ECGI.

Geometric alignment of the EAM and computed tomography geometries is challenging but was optimized by using fixed anatomic landmarks, as well as ensuring no geometric shifts on CARTO during data collection. However, as demonstrated by our in-depth analysis, EAM-ECGI comparison is intrinsically sensitive to small variations in the anatomical coregistration. This could also have affected the distance measurements garnered from localization of the pacing points. EAM and ECGI systems estimate the reference potential of unipolar electrogram in a slightly different way, which may have reduced the morphological correlation. This study did not focus on the accuracy of ventricular arrhythmia localization which is the subject of ongoing work.

Conclusions

There is a moderate correlation between reconstructed electrograms recorded using ECGI and contact unipolar electrograms recorded from the epicardium during catheter ablation of VT in patients with structural heart disease. ECGI and contact electrogram correlations are sensitive to electrode apposition and geometric alignment. Further technological developments may improve spatial resolution and electrogram correlations.

ARTICLE INFORMATION

Received December 11, 2018; accepted March 5, 2019.

The Data Supplement is available at https://www.ahajournals.org/doi/suppl/10.1161/CIRCEP.118.007120.

Authors

Adam J. Graham, MRCP*; Michele Orini, PhD*; Ernesto Zacur, PhD; Gurpreet Dhillon, MRCP; Holly Daw, MSc; Niel T. Srinivasan, MRCP; Jem D. Lane, PhD, MRCP; Alex Cambridge, BSc; Jason Garcia, BSc; Nanci J. O'Reilly, MBBS; Sarah Whittaker-Axon, BSc; Peter Taggart, MD, DSc; Martin Lowe, PhD, FRCP; Malcolm Finlay, PhD, MRCP; Mark J. Earley, MD, FRCP; Antony Chow, MD, MRCP; Simon Sporton, MD, FRCP; Mehul Dhinoja, MD, MRCP; Richard J. Schilling, MD, MRCP; Ross J. Hunter, MRCP, PhD; Pier D. Lambiase, PhD, FRCP

Correspondence

Pier D. Lambiase, PhD, UCL Institute of Cardiovascular Science and Cardiology Department, Barts Heart Centre, Barts Health NHS Trust, W Smithfield, London, EC1A 7BE, United Kingdom. Email p.lambiase@ucl.ac.uk

Affiliations

Barts Heart Centre, Barts Health NHS Trust, London, United Kingdom (A.J.G., M.O., G.D., H.D., N.T.S., J.D.L., A. Cambridge, J.G., N.J.O., S.W.-A., M.L., M.F., M.J.E., A. Chow, S.S., M.D., R.J.S., R.J.H., P.D.L.). Department of Mechanical Engineering (M.O.) and Institute of Cardiovascular Science (P.T., P.D.L.), University College London, United Kingdom. Institute of Biomedical Engineering, University of Oxford, United Kingdom (E.Z.).

Sources of Funding

A. Graham is supported by Barts Charity. Dr Orini is supported by British Heart Foundation (BHF) grant PG/16/81/32441. Dr Lambiase is supported by University College London Hospitals Biomedicine National Institute of Health Research (UCLH Biomedicine NIHR) and Barts British Research Centre (BRC). The study was in part supported by a Medtronic External Research Program grant.

Disclosures

None.

REFERENCES

1. Oster HS, Taccardi B, Lux RL, Ershler PR, Rudy Y. Electrocardiographic imaging: noninvasive characterization of intramural myocardial activation from inverse-reconstructed epicardial potentials and electrograms. *Circulation.* 1998;97:1496–1507.
2. Burnes JE, Taccardi B, Rudy Y. A noninvasive imaging modality for cardiac arrhythmias. *Circulation.* 2000;102:2152–2158.
3. Dubois R, Shah AJ, Hocini M, Denis A, Derval N, Cochet H, Sacher F, Bear L, Duchateau J, Jais P, Haissaguerre M. Non-invasive cardiac mapping in clinical practice: application to the ablation of cardiac arrhythmias. *J Electrocardiol.* 2015;48:966–974. doi: 10.1016/j.jelectrocard.2015.08.028
4. Rudy Y. Noninvasive electrocardiographic imaging of arrhythmogenic substrates in humans. *Circ Res.* 2013;112:863–874. doi: 10.1161/CIRCRESAHA.112.279315
5. Zhang J, Cooper DH, Desouza KA, Cuculich PS, Woodard PK, Smith TW, Rudy Y. Electrophysiologic scar substrate in relation to VT: noninvasive high-resolution mapping and risk assessment with ECGI. *Pacing Clin Electrophysiol*. 2016;39:781–791.

6. Ghosh S, Rudy Y. Accuracy of quadratic versus linear interpolation in noninvasive electrocardiographic imaging (ECGI). *Ann Biomed Eng*. 2005;33:1187–1201.
7. Ramanathan C, Jia P, Ghanem R, Ryu K, Rudy Y. Activation and repolarization of the normal human heart under complete physiological conditions. *Proc Natl Acad Sci USA*. 2006;103:6309–6314.
8. Burnes JE, Ghanem RN, Waldo AL, Rudy Y. Imaging dispersion of myocardial repolarization, I: comparison of body-surface and epicardial measures. *Circulation*. 2001;104:1299–1305.
9. Ghanem RN, Jia P, Ramanathan C, Ryu K, Markowitz A, Rudy Y. Noninvasive electrocardiographic imaging (ECGI): comparison to intraoperative mapping in patients. *Heart Rhythm*. 2005;2:339–354.
10. Jamil-Copley S, Bokan R, Kojodjojo P, Qureshi N, Koa-Wing M, Hayat S, Kyriacou A, Sandler B, Sohaib A, Wright I, Davies DW, Whinnett Z, Peters NS, Kanagaratnam P, Lim PB. Noninvasive electrocardiographic mapping to guide ablation of outflow tract ventricular arrhythmias. *Heart Rhythm*. 2014;11:587–594. doi: 10.1016/j.hrthm.2014.01.013
11. Yamashita S, Shah AJ, Mahida S, Sellal JM, Berte B, Hooks D, Frontera A, Jefairi NA, Wielandts JY, Lim HS, Amraoui S, Denis A, Derval N, Sacher F, Cochet H, Hocini M, Jaïs P, Haïssaguerre M. Body surface mapping to guide atrial fibrillation ablation. *Arrhythm Electrophysiol Rev*. 2015;4:172–176. doi: 10.15420/aer.2015.4.3.172
12. Cuculich PS, Schill MR, Kashani R, Mutic S, Lang A, Cooper D, Faddis M, Gleva M, Noheria A, Smith TW, Hallahan D, Rudy Y, Robinson CG. Noninvasive cardiac radiation for ablation of ventricular tachycardia. *N Engl J Med*. 2017;377:2325–2336.
13. Robinson CG, Samson PP, Moore KMS, Hugo GD, Knutson N, Mutic S, Goddu SM, Lang A, Cooper DH, Faddis M, Noheria A, Smith TW, Woodard PK, Gropler RJ, Hallahan DE, Rudy Y, Cuculich PS. Phase I/II trial of electrophysiology-guided noninvasive cardiac radioablation for ventricular tachycardia. *Circulation*. 2019;139:313–321. doi: 10.1161/CIRCULATIONAHA.118.038261
14. Cluitmans MJM, Bonizzi P, Karel JMH, Das M, Kietselaer BLJH, de Jong MMJ, Prinzen FW, Peeters RLM, Westra RL, Volders PGA. *In Vivo* validation of electrocardiographic imaging. *JACC Clin Electrophysiol*. 2017;3:232–242. doi: 10.1016/j.jacep.2016.11.012
15. Bear LR, LeGrice IJ, Sands GB, Lever NA, Loiselle DS, Paterson DJ, Cheng LK, Smaill BH. How accurate is inverse electrocardiographic mapping? *Circ Arrhythm Electrophysiol*. 2018;11:e006108.
16. Sapp JL, Dawoud F, Clements JC, Horáček BM. Inverse solution mapping of epicardial potentials: quantitative comparison with epicardial contact mapping. *Circ Arrhythm Electrophysiol*. 2012;5:1001–1009.
17. Duchateau J, Sacher F, Pambrun T, Derval N, Chamorro-Servent J, Denis A, Ploux S, Hocini M, Jaïs P, Bernus O, Haïssaguerre M, Dubois R. Performance and limitations of noninvasive cardiac activation mapping. *Heart Rhythm*. 2019;16:435–442. doi: 10.1016/j.hrthm.2018.10.010
18. Sosa E, Scanavacca M, d'Avila A, Pilleggi F. A new technique to perform epicardial mapping in the electrophysiology laboratory. *J Cardiovasc Electrophysiol*. 1996;7:531–536.
19. Coronel R, de Bakker JMT, Wilms-Schopman FJG, Opthof T, Linnenbank AC, Belterman CN, Janse MJ. Monophasic action potentials and activation recovery intervals as measures of ventricular action potential duration: experimental evidence to resolve some controversies. *Heart Rhythm*. 2006;3:1043–1050.
20. Orini M, Taggart P, Lambiase PD. In vivo human sock-mapping validation of a simple model that explains unipolar electrogram morphology in relation to conduction-repolarization dynamics. *J Cardiovasc Electrophysiol*. 2018;29:990–997.
21. Orini M, Taggart P, Srinivasan N, Hayward M, Lambiase PD. Interactions between activation and repolarization restitution properties in the intact human heart: in-vivo whole-heart data and mathematical description. *PLoS One*. 2016;11:e0161765.
22. Martin CA, Orini M, Srinivasan NT, Bhar-Amato J, Honarbakhsh S, Chow AW, Lowe MD, Ben-Simon R, Elliott PM, Taggart P, Lambiase PD. Assessment of a conduction-repolarisation metric to predict Arrhythmogenesis in right ventricular disorders. *Int J Cardiol*. 2018;271:75–80. doi: 10.1016/j.ijcard.2018.05.063
23. Ramanathan C, Rudy Y. Electrocardiographic imaging: II. Effect of torso inhomogeneities on noninvasive reconstruction of epicardial potentials, electrograms, and isochrones. *J Cardiovasc Electrophysiol*. 2001;12:241–252.
24. Rudy Y. Noninvasive ECG imaging (ECGI): mapping the arrhythmic substrate of the human heart. *Int J Cardiol*. 2017;237:13–14. doi: 10.1016/j.ijcard.2017.02.104
25. Ghanem RN, Burnes JE, Waldo AL, Rudy Y. Imaging dispersion of myocardial repolarization, II: noninvasive reconstruction of epicardial measures. *Circulation*. 2001;104:1306–1312.
26. Oster HS, Taccardi B, Lux RL, Ershler PR, Rudy Y. Noninvasive electrocardiographic imaging: reconstruction of epicardial potentials, electrograms, and isochrones and localization of single and multiple electrocardiac events. *Circulation*. 1997;96:1012–1024.
27. Ramanathan C, Jia P, Ghanem R, Calvetti D, Rudy Y. Noninvasive electrocardiographic imaging (ECGI): application of the generalized minimal residual (GMRes) method. *Ann Biomed Eng*. 2003;31:981–994.
28. Revishvili AS, Wissner E, Lebedev DS, Lemes C, Deiss S, Metzner A, Kalinin VV, Sopov OV, Labartkava EZ, Kalinin AV, Chmelevsky M, Zubarev SV, Chaykovskaya MK, Tsiklauri MG, Kuck KH. Validation of the mapping accuracy of a novel non-invasive epicardial and endocardial electrophysiology system. *Europace*. 2015;17:1282–1288. doi: 10.1093/europace/euu339
29. Tung R, Josephson ME, Bradfield JS, Shivkumar K. Directional influences of ventricular activation on myocardial scar characterization: voltage mapping with multiple wavefronts during ventricular tachycardia ablation. *Circ Arrhythm Electrophysiol*. 2016;9:e004155.
30. Glashan CA, Androulakis AFA, Tao Q, Glashan RN, Wisse LJ, Ebert M, de Ruiter MC, van Meer BJ, Brouwer C, Dekkers OM, Pijnappels DA, de Bakker JMT, de Riva M, Piers SRD, Zeppenfeld K. Whole human heart histology to validate electroanatomical voltage mapping in patients with non-ischaemic cardiomyopathy and ventricular tachycardia. *Eur Heart J*. 2018;39:2867–2875. doi: 10.1093/eurheartj/ehy168
31. Cluitmans M, Brooks DH, MacLeod R, Dössel O, Guillem MS, van Dam PM, Svehlikova J, He B, Sapp J, Wang L, Bear L. Validation and opportunities of electrocardiographic imaging: from technical achievements to clinical applications. *Front Physiol*. 2018;9:1305. doi: 10.3389/fphys.2018.01305
32. Tschabrunn CM, Roujol S, Dorman NC, Nezafat R, Josephson ME, Anter E. High-resolution mapping of ventricular scar: comparison between single and multielectrode catheters. *Circ Arrhythm Electrophysiol*. 2016;9:e003841.